IEEE Access
Multidisciplinary | Rapid Review | Open Access Journal

Received 21 October 2024, accepted 9 November 2024, date of publication 2 December 2024, date of current version 19 December 2024.

Digital Object Identifier 10.1109/ACCESS.2024.3509689

RESEARCH ARTICLE

The Design and Optimization of Additively Manufactured Windings Utilizing Data Driven Algorithms for Minimal Loss in Electric Machines

JOHN MCKAY[1], (Member, IEEE), JILL MISCANDLON[2], AND TATYANA KONKOVA[1]
[1]Department of Design, Manufacturing and Engineering Management, University of Strathclyde, G1 1XQ Glasgow, U.K.
[2]National Manufacturing Institute Scotland, University of Strathclyde, G1 1XQ Glasgow, U.K.

Corresponding author: John Mckay (John.mckay@strath.ac.uk)

This research is funded solely by the National Manufacturing Institute Scotland, Industrial Doctorate Centre, which is part of the University of Strathclyde. The work undertaken is linked to the Engineering and Physical Sciences Research Council of the UK Future Electrical Machines Manufacturing Hub (EP/S018034/1).

ABSTRACT Permanent magnet (PM) electrical machines are an ever increasingly utilised motor topology for numerous industries such as automotive, aerospace, manufacturing, energy and premium consumer goods. PM electrical machines exhibit high power density, high operating efficiency and high torque to current ratio, whilst remaining robust and fault tolerant. However, the stator windings account for a significant proportion of the overall motor losses. There are many avenues for machine designers to potentially reduce winding losses whilst increasing overall efficiency and performance. Such avenues include, thermal management systems, novel winding materials and novel winding manufacturing methods. Additive manufacturing is generally recognised as a transformative manufacturing technology, especially in the design of electric machines. The ability to create a wide array of geometric shapes offers a level of design freedom that was previously unattainable. Additive manufacturing is therefore utilised in this paper to produce novel, optimised winding designs that have been configured to minimise total machine loss and maximise machine efficiency. This paper investigates the use of an algorithmic optimisation process within Ansys Optislang, and automated using python scripting. The optimisation process consists of sensitivity analysis utilising an efficient hybrid 2D FEA-Analytical model, meta-modelling and genetic algorithm to search the design space for optimal winding designs. The optimal designs are then validated against 2D and 3D FEA high precision motor models within Ansys maxwell and MotorCad and compared against a benchmark winding configuration. It was found that the most optimal winding design produced a motor efficiency of 97%.

INDEX TERMS Additive manufacturing, aerospace industry, automotive industry, design optimization, electric motors, Eddy current losses, genetic algorithms, machine windings, optimization, PMSM.

I. INTRODUCTION

Permanent magnet (PM) electrical motors are an ever increasingly utilised motor topology for numerous industries such as automotive, aerospace, manufacturing, energy and premium consumer goods [1]. This is due to their superior characteristics over other topologies that include; high power density, high efficiency across the range of operation, high starting torque, high torque to current ratio, wide speed range, constant power operation, high intermittent overload capabilities, reliability and robustness, and low acoustic noise and vibration [1], [2], [3].

Over the past few decades, there has been a shift towards hybrid and fully electric drive trains for vehicles and

The associate editor coordinating the review of this manuscript and approving it for publication was Shadi Alawneh.

transportation in order to reduce emissions and to create a sustainable environment with reduced dependency on fossil fuels [3].

Permanent Magnet Synchronous Motors (PMSM) are being readily used for automotive traction systems with electric vehicle adoption increasing. In terms of aviation, research and industrial projects are currently being undertaken to utilise the topology for aerospace applications, especially civilian air transportation, where emissions account for 12% of the global annual emissions output with the number of passengers set to double by 2035 [4]. The PMSM topology is under consideration for starter generator applications and for high power alternative propulsion systems as part of MEA (More Electric Aircraft) and HEA (Hybrid Electric Aircraft) concepts for high efficiency, power density and robustness. This is part of the EU commission policy report ''Flightpath 2050'' which aims to reduce aviation CO2 emissions by 75%, NOx by 90% and noise by 65% by 2050 [5].

Another area of concern regarding the efficiency of electrical machines is global electrical energy consumption. It is becoming increasingly important to continue to improve upon motor efficiency in a broader domestic and industrial sense. As of 2009 onwards, the European Commission Regulation (EC) No 640/2009, has meant that continuous incremental improvements in electrical machines has contributed effectively to low carbon economy targets, set by the European Union.

The eco-design requirements regulation by the EU was subsequently updated on the 1st of July 2021, with a broader scope to include single speed 50Hz/60Hz induction motors. The regulation also includes variable speed drives and requires all variable speed drives to reach at least IE level 2 efficiency and three phase motors with rated power between 0.75Kw and 200Kw must meet IE level 4 by July 2023. The IE standard is the ratios of Mechanical Output power to the electrical input power and includes other machine characteristics in its standard.

The EU is the first place worldwide to make IE level 4 Mandatory for some motors. It is postulated, that 50% of the worlds electrical energy consumption is consumed by electrical motors. (Commission Regulation (EU) 2021/341) [6].

II. MOTIVATION FOR WINDING OPTIMISATION

The stator windings in PMSM's often account for the largest proportion of total machine losses [7]. Winding loss within a PM motor can be defined by two basic components: DC and AC power loss. The presence of both DC and AC loss effects makes winding design complex, as a balance needs to be struck between the DC and the AC loss mechanisms. Both DC and AC behaviour are linked directly to the geometric configuration of the conductors in the winding. Whilst DC power loss components and thermal dependence is well understood and used to estimate machine performance, AC loss components are difficult to compute accurately as they are a direct function of the winding's individual conductor geometry, layout and operating frequency [8].

Motor designers typically only take into account the DC losses in the design process. This is because modelling and simulating the AC loss components is computationally heavy and time consuming. However, sufficiently high AC frequency operation can have a significant effect on the loss behaviour of the device, due to the presence of eddy currents [9].

Fill factor has been traditionally used as an umbrella metric for low loss winding performance. A winding design with a high fill factor was commonly seen as ''good'', however as stated, there are a plethora of other effects to take into account. AC effects such as skin effects and proximity effects also need to be accounted for. These additional effects scale with operating frequency, further complicating the winding design philosophy as conductor profiles, arrangement and lay in the stator slots become ever increasingly important [10].

III. NOVEL WINDING MANUFACTURING METHODS

Novel manufacturing technologies and processes are enabling the manufacture of unique winding designs that may offer benefits in terms of performance and loss mitigation. Some recent examples in literature include metal casted windings developed by Fraunhofer, illustrating the casting of aluminium and copper windings. Whilst electrical conductivity is conserved when compared to their raw material counterparts, the winding geometry appears limited to flat, trapezoidal conductor shapes with low numbers of turns. Minimal conductor heights of 0.7 mm can be achieved, with achievable winding lengths of 200 mm demonstrated. The process is limited to concentrated windings, with conductor shaping hindering AC loss minimisation to effects such as proximity and skin effects [11], [12].

Forming is a cost and energy effective solution, generating little waste material and low equipment costs. Present types of forming processes such as compression, rolling and pressing have been demonstrated. The trapezoidal windings are a good candidate for such a process, however there are drawbacks due to high degrees of deformation, including insulation application, reduction in achievable fill factors, surface quality, limited conductor shaping and burr formation [13]. For milling, KITECH has been manufacturing high fill factor trapezoidal windings using milling, accomplished with CNC machines. Once milled, the windings are insulated and compressed to fit into the slot. However, the processes suitability for mass production is limited and therefore only small batches and prototypes are created. Such a process may be of interest for the aerospace industry, where cost constraints are less of a limiting factor [12]. A novel processing chain has been developed by Fraunhofer to increase the slot fill factor and to enable unique geometry by processing each section of wire sequentially to allow for adaptive geometry on a per turn basis. The process consists of a pressing tool, immersion elements, bending and pressing jaws. However, the process does have some disadvantages,

including technical challenges involving wire guiding that result in alternating displacement of the wire axis, increased gapping between winding sections and burr formations [14].

Some previous examples in literature include, pre-cut foil windings [15], forming bobbin shaped windings using traditional round wires [16] and stacked printed circuit board-based arrangements connected electrically at the windings or by busbar [17].

One manufacturing technology that is receiving significant attention is the use of additive manufacturing (AM) in winding design. The ability for additive manufacturing to create unconstrained three-dimensional and novel geometries which would not be possible via traditional manufacturing methods is an exciting development. The potential to print; a variety of materials including plastics, ceramics, metal alloys and even biological material through, rapid prototyping, combined with little to no materials waste, makes additive manufacturing a highly attractive technology. Recent research has focussed on the use of additive manufacturing for electric motors and their components. There are many different examples of AM such as selective laser melting (SLM), electron beam melting (EBM), 3D screen printing [18], 3D multi-material printing [19] and wire-cut electrical discharge machining [20]. The use of 3D multi-material printing is especially interesting with its ability to print both conductive and ceramic insulation material simultaneously [21].

As of 2018 the additive manufacturing industry as a whole (referring to the inclusion of hardware, software, materials, production and includes industries such as aerospace, health care and automotive) was worth approximately $9.3 billion dollars. This is expected to rise to $41.1 billion dollars by 2027 [10]. Companies such as Airbus and BMW are already utilising additive manufacturing in rapid production prototyping and high-volume production for aerospace and automotive [10], [22]. Additive manufacturing has been recognised as *a key enabling technology for many industries*. Coupled with advances in high precision and high-fidelity electromagnetic computation, the technology offers opportunities to design solutions that would otherwise be considered too challenging, costly or impossible to produce using conventional manufacturing techniques [2], [10], [23], [24].

IV. TRENDS IN WINDING OPTIMISATION

There is a trend in published literature towards the precise placement and shape of each turn of a winding having a distinct shape, produced by non-conventional manufacturing technologies, for example additive manufacturing [25]. Various types of conductor shapes have been explored previously such as trapezoidal or flat conductors, which allow for high fill factor and high current density, however, suffer significantly in AC high speed operation. Attempts have been made to alleviate this challenge by shaping each winding turn by aligning the conductors with the flux lines, therefore avoiding high gradients of magnetic vector potential produced by the magnetic material on the rotor, thus reducing the conductor's exposure to leakage flux [2]. Multi-material 3D printing has allowed for the simultaneous printing of flat and circular conductors surrounded by ceramic insulation material, however the fill factors achieved are low at 33.8% and the number of turns achieved are also low at just 10 and 14 turns. Flat, trapezoidal and circular conductors manufactured in this way also appear limited to concentrated windings [21], [26].

The use of integrated heat pipes directly placed into additively manufactured windings has also been utilised to increase the integrity of the insulation by targeting winding hot spots. The operational lifetime of an electric motor depends largely on the insulation. High power machines use direct liquid cooling, typically consisting of ethanol-glycol to control temperature [27], [28]. Fan Wu et al. demonstrate that cooling pipe placement should be a strategic decision and not generic in nature. The upper most winding turns exposed to the leakage flux produced by the armature field, generate more joule losses. It was shown that by reducing those conductors' cross section and by introducing cooling pipes for those conductors helped reduce losses at sufficiently high operational frequencies.

The use of hybridised conductor windings containing a mixture of solid and stranded conductors that make up a winding. Solid conductors may exhibit higher AC losses compared to stranded conductors at sufficiently high operational frequencies. Conductors situated at the top of the slot are especially affected by proximity effect from leakage flux generated by the magnetic material on the rotor iron [2]. Simpson et al., demonstrates the use of replacing the solid conductors near the top of the slot with stranded conductors to reduce the proximity effect experienced by those turns affected. However, not every strand is exposed to the same magnitude of magnetic field, altering their independences on a per strand basis. Transposition in the end windings was introduced to avoid circulating currents between strands. The limitation is that parallelised conductors must remain relatively large in terms of size and the number of parallel strands is limited to four per turn, due to the limitations of the additive manufacturing process. These features limit the stranded turn's ability to run at high operational frequencies due to AC loss mechanisms such as proximity and skin effects, however, transposition is achieved in the end winding sections. Smaller and more numerous parallel strands would help with these challenges but were no doubt deemed unfeasible to manufacture. The presence of the turns at the top of the slot also makes those conductors susceptible to leakage flux and thus joule losses incurred due to armature reaction.

A clear trend in literature is that windings manufactured using AM appear to be concentrated in nature as manufacturing a distributed winding may be challenging to realise practically. In order to improve the performance of a PMSM machine concentrating on winding loss performance, novel ideas have been published that make use of solid

conductors rather than traditional stranded circular wire windings. The leveraging of more advanced manufacturing technologies enables more sophisticated winding geometries to be designed and optimised. Conventional windings use round or square drawn copper wire windings for the stator windings. The windings within this research paper cannot be manufactured by traditional winding processes due to the requirement of different conductor shape, size, orientation and position. Each turn within the winding can be entirely unique.

This research paper contributes to the literature by presenting windings optimised via an automated algorithmic optimisation process, utilising a unique structure that includes sensitivity analysis and meta-modelling, followed by a multi-objective genetic algorithm (MOGA) to search the design space. It consists of Ansys Optislang connected directly via numerous custom python scripting packages to a hybrid 2D custom finite element analysis with analytical elements model of a PMSM motor for time and compute efficiency. Thermal and mechanical modelling are pre-computed within Ansys MotorCAD and Lumped Parameter Thermal Models (LPTN's) are utilised to dictate material behaviour at simulated temperatures.

The resulting windings attempt to balance the Rac/Rdc, a well-known engineering trade-off at a singular operating point of 1500 RPM. The windings designed attempt to maximise fill factor, whilst minimise DC and AC effects such as proximity and skin effects. The design freedoms afforded by additive manufacturing also allows the process to place conductors meaningfully to attempt to avoid armature field joule losses incurred by leakage flux. The research offers unique winding arrangements not previously seen in literature with unique conductor cross sections such as triangles and hexagons to be placed meaningfully within the slot to minimise losses whilst increasing efficiency. It was observed that overall motor efficiency was increased by around 6-7% when compared to a benchmark winding design. Weight savings of up to 1.48 kg for concentrated windings and 4.88 kg for distributed windings were observed, reducing winding mass and increasing motor power density. The maximal motor efficiency achieved was 97% using the optimisation process developed.

V. OPTIMISATION OF ELECTRIC MOTORS

Electric motor designers have been utilising optimisation of electrical machines for decades. Because of the many parameters being optimised, it is viewed mostly as a multi-objective scenario as there are many goals being optimised for [29]. With the rise in demand for more efficient, compact, lighter and cost-effective electric motor solutions, multiphysics design optimisation strategies are becoming increasingly attractive at the early stages of the motor design process. The machine design industry has developed rapidly in recent years due to the electrification of transportation. This creates a challenge for designers within industries such as automotive where they are incentivized to design motors with high power and torque whilst retaining the feasibility of mass production. Furthermore, the project turnaround for machine design is becoming shorter and so automated optimisation processes are becoming more indispensable [30]. Engineering designs are generally broken down into two distinct parts, modelling and optimisation. Modelling techniques typically include analytical or lumped parameter models, numerical methods and finite element analysis. Optimisation algorithms are classified as either deterministic or stochastic, which is the exploration of the design space either systematically or randomly [31].

Deterministic optimisation aims to find the best global optima with certainty, utilising algorithms that provide theoretical guarantees that the returned result is the best solution. Stochastic methods use a random search of the optimisation space utilising algorithms such as evolutionary [32], [33], genetic [34], [35] or particle swarm algorithms [36], [37]. Deterministic optimisation however is computationally intensive and time consuming, whilst stochastic modern optimization methods offer advantages over deterministic methods as They are less prone to getting trapped in local optima and can handle large numbers of variables or parameters. This approach to engineering optimization scenarios has a distinct advantage with multi-physics problems [29]. The trapping of deterministic optimisation is termed as the 'step-size problem', and is a well-known disadvantage to deterministic optimisation strategies, where a finer stepping to explore search areas of interest compound search time and deplete computational resources. This contrasts with stochastic methods which are gradient free and possess a continuously evolving population of potential solution candidates [31].

Optimisation algorithms are evaluated based on three principles: accuracy, robustness and efficiency. The features all oppose one another with an example being robustness which is slow, forcing a trade-off between convergence, storage, robustness and speed. Space reduction is used with the aim of reducing the number of function evaluations [38]. Two common methods for motor optimisation is DOE, design of experiments and stochastic evolutionary algorithms, especially for significant dimensional parameters [39], [40].

For design optimisation tasks coupled with FEA, such as the process presented in this paper, the most important feature after accuracy is efficiency, therefore trading robustness for computational time and function evaluations [38]. Computationally Efficient Finite Element Analysis (CEFEA) exploits existing electrical symmetry and magnetic periodicity of PMSM topologies with sinusoidal excitation. With CEFEA it is possible to reduce computational time by up to two orders of magnitude [38]. It was necessary to adopt a CEFEA approach, due to the complex nature of winding interaction that cannot be analysed analytically with the highly complex structures presented within this paper.

Since the number of variables multiplies the number of experiments and optimisation time, it is required to decrease

the design space by reducing the number of variables. Sensitivity analysis is a commonly used approach in motor design. Sensitivity analysis represents the first step in the optimisation process detailed in this paper, where the hybrid analytical-FEA motor model is used and developed with CEFEA in mind to evaluate how meaningful the input variables, in this case, each of the individual conductors' position, shape, size and rotation has on the output of the PMSM motor model.

Space reduction in electric motor optimisation involves decreasing the dimensionality of the search space to enhance firstly computational efficiency and secondly, simplifying the optimisation process. This includes selecting the most relevant variables, reducing the number of constraints and using a simplified model, often referred to as a ''surrogate''. Techniques such as surrogate modelling are employed to focus on the most influential parameters and approximate complex behaviours with fewer computations. By targeting a reduced set of key design variables and using efficient search algorithms such as genetic algorithms, space reduction enables quicker convergence to high-quality solutions, making the optimisation process more tractable while maintaining performance standards. To assess the quality of a surrogate model, the use of the coefficient of optimal prognosis was used to determine the quality of the model before being utilised by the genetic algorithm [30], [41].

In this case a meta-model (the Meta-Model of Optimal Prognosis) surrogate model is used to represent a decreased dimensionality model of the variables being altered. In this paper, given the sheer number of variables representing a windings configuration (approximately 240), it was necessary to alter a minimal set of variables per optimisation pass, termed in this paper as an optimisation 'stage', where each of the 48 conductors would have their positions altered firstly, then size, shape and orientation. By reducing the number of variables being utilised per optimisation pass, the quality of the meta-model increases, giving a higher quality representation of the phenomena being represented. Each successive result would seed the next optimisation stage. Meta-modelling represents the second step in the overall optimisation process.

Optimisation algorithms rely on an equivalent model, or 'surrogate model' for obtaining fitness values, which depends heavily on the accuracy of the modelling involved. Using genetic algorithms, thousands of designs are evaluated, per optimisation run in order to solve high-dimensional design problems. Therefore, modelling speed is an important criterion for design optimisation involving many different design parameters [32]. Such as those seen in this paper.

Multi-objective, constrained optimisation genetic algorithms, referred to as MOGA [31], are designed for optimisation scenarios where there are conflicts with objectives and constraints. These algorithms facilitate the evaluation of solutions through various fitness functions to identify a set of optimal solutions positioned upon a pareto front, which represent a balance between multiple criteria of interest. Unlike single- objective optimisation methods, multi-objective constrained genetic algorithms are designed to maintain a diverse candidate population throughout the iteration process. This guarantees a comprehensive exploration of the design space and effectively captures the trade-offs between conflicting objectives. This results in the identified solutions on the pareto front, ultimately adhere to the specified constraints [32]. In this paper once the optimal designs are found, they are validated against via a 2D FEA simulation. Further validation of winding designs of interest were compared against full 3D FEA simulations for greater precision and accuracy.

There are many different examples in literature of the use of optimisation algorithmic processes in electric motor design. For example, motor topology optimisation [37], geometry optimisation [29], [36], operating point optimisation [42], [43], winding optimisation [25], [35] and materials [36] optimisation to name a few.

A general criticism of optimisation-based designs is that it is easy to lose track of the actual optimisation process itself, and therefore, useful engineering insights are often lost from the design. This criticism was challenged in this research by the splitting of the optimisation process into unique stages allowing for deeper consideration of why certain optimisations and therefore structures were being developed by the process [32].

VI. PROBLEM DEFINITION

Consider an empty open slot within the stator of a PMSM motor, as shown in Figure 1. An open slot topology was chosen because it is favourable in the use of prefabricated, pre-processed windings such as those manufactured by AM [44].

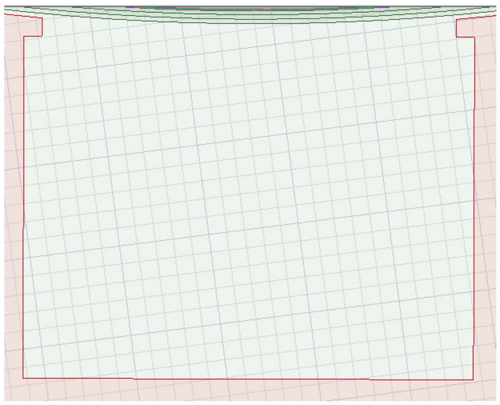

FIGURE 1. An empty stator slot.

Most machine designers use DC performance when designing a winding due to the complexities and computational effort in modelling AC effects [9]. As can be seen in Dowels equation (1), many of the terms are fixed, and linear assumptions are made about conductor cross-section, the number of layers, diameter and thickness. Whilst analytical

methods for modelling loss effects within a winding are efficient at estimating losses within the conductors, a clear disadvantage is the need for those analytical models to be reformulated when a machine topology changes. For example, they assume linear magnetically permeable materials, fixed machine topologies, but more importantly, assume conductor placements and layouts within the available stator slot space that are repeatable in terms of shape, dimensions, spacing and layering, and therefore, limit design freedom [23].

$$K = \frac{R_{ac}}{R_{dc}} = Re\{\alpha.h.\coth(\alpha.h)\} + \frac{m^2-1}{3}.Re\left\{2.\alpha.tanh\left(\frac{\alpha.h}{2}\right)\right\} \quad (1)$$

Two time stepped electromagnetic models were developed. A concentrated single layered winding and a distributed dual layered winding. Both motor topologies and winding layouts were developed firstly in MotorCAD and comprised of a benchmark winding layout that was used to compare performance against the algorithmically generated designs. Both models contained identical parameters for motor topology and winding layout within the slot. Figure 2 shows the benchmark winding layout in Ansys MotorCAD on the left and the replicated benchmark winding in the hybrid Ansys Maxwell model on the right. The winding layout was identical for both the concentrated and distributed benchmark windings.

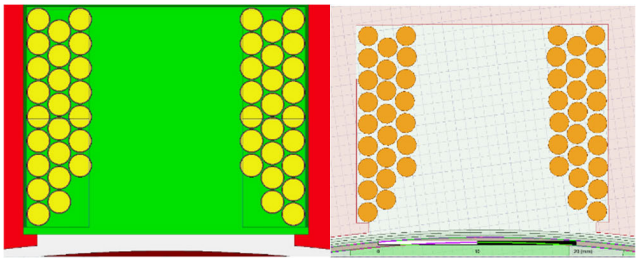

FIGURE 2. (L) The benchmark winding in MotorCAD, and (R) the benchmark winding replicated in Ansys Maxwell.

TABLE 1. Benchmark design parameters at 20°C operating temperatures.

parameters	Concentrated winding machine	Distributed winding machine
Phases	3	3
Winding throw	1	3
Parallel branches	4	4
Winding layers	1	2
No of conductors per slot	48	48
Slot number	24	24
Pole number	28	28
Stator diameter (mm)	208	308
Stator length (mm)	210	210
Motor length (mm)	340	340
Slot width (mm)	25	25
Slot height (mm)	20	20
Tooth tip height (mm)	1	1
Machine speed (RPM)	1500	1500
Benchmark winding efficiency @ 20^0C (%)	92.276	88.233
Benchmark winding Total losses @ 20^0C (W)	13887	153082

In order to achieve a high level of conductor layout customisation, the MotorCad models were then developed and parameterised in the hybrid Ansys Maxwell model, where automation could be utilised to place conductors of varying shape, size, position and orientation within the predetermined slot space of phase A in the model. Both the concentrated and distributed hybrid Ansys Maxwell models were tested and validated by constructing the benchmark winding layout structure in their respective hybrid Ansys Maxwell models. The losses observed were then compared against losses observed in their MotorCad equivalents. This ensured a high level of accuracy, and that both the MotorCad version of the models and their equivalent hybrid Ansys Maxwell models were in agreement with measured values of loss before the algorithmically generated winding models were compared.

In terms of end winding behaviour, the hybrid Ansys Maxwell models simulates the active winding sections only, *i.e.* the parts of the winding encompassed within the stator slot. The end windings could be modelled as external circuits with known value of resistance and inductances, however, with the large number of simulations taking place (approximately 25,000) it would be impossible to know all specific values of resistances and inductances for every custom windings end winding behaviour. Therefore, an assumption is made, that the behaviour of the end winding is predominantly DC loss. This assumption is validated and tested with a high precision 3D model of two concentrated winding designs, #834 and #9354. For clarity, windings were named by their simulation number and begin with a '#' prefix. It can be posited that as long as the end windings are no longer than 50% of the active winding sections, then AC loss mechanisms such as Skin effects can therefore be neglected [45]. In order to simulate as many winding designs as possible it was necessary to have a highly time efficient FEA model that allowed maximal winding layout freedom whilst retaining high precision. It was decided that the number of conductors composing the winding would be fixed to 48 per slot.

A concentrated winding consumed 2 slots, whilst a distributed winding consumed 4 half slots (at 2 windings per slot), whilst still containing 48 conductors. To reduce the number of variables being altered at any one time, a winding would be designed in one slot space like in Figure 3 and then mirrored to complete the winding in the adjacent slot. This approach helped reduce computation time and end winding model complexity. Distributed windings would have the top parts of the winding be identical and the bottom parts of the winding following the same pattern. This simplified the design process and the generated FEA model, as a distributed winding could be designed and represented in an identical number of conductors to the concentrated winding. A total of 48 conductors were chosen as it was easily divisible by many integers, but also when drawing the geometry in the two-dimensional hybrid Ansys Maxwell model, it kept the complex geometry to a minimal of 96 high precision, full geometry conductors. Through experimentation, it was found that 96 conductors were computationally efficient as

utilising more high precision full geometry conductors to represent a winding, whilst possible, slowed computation down from ∼2-3 minutes to 30-45 minutes, even on modern high-performance computer hardware.

VII. HYBRID FEA-ANALYTICAL MOTOR MODEL

The hybrid Ansys Maxwell model, is an FEA electromagnetic model that uses a mixture of analytical winding representations, and one fully formed geometrically complex winding associated with phase A of the electrical input. By utilising the CEFEA concept, symmetry is also utilised to save on computational time.

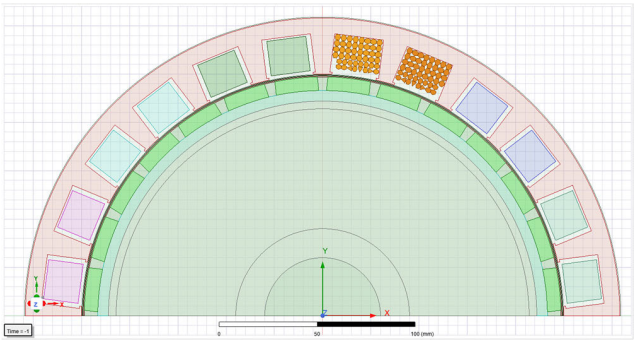

FIGURE 3. The hybrid model.

As can be seen in Figure 3, only one winding is represented in full high precision geometry. The rest of the windings comprise of analytically modelled windings represented by colour coded squares associated to their respective phases. For the analytical winding representations, the following assumptions were made:

- Assumed 100% fill factor
- Current density is assumed to be uniform
- Conductors are repeatable, uniformly shaped, with uniform spacing and uniform cross-sections
- Inductances and resistances are computed by the solver
- Analytically represented windings do not consider complex loss mechanisms such as skin effects and proximity effects
- End winding losses are not computed, only active model sections.

The complex winding geometry allowed the study of both DC loss and AC loss mechanisms such as skin, proximity effects and armature reaction. The model was excited via 3-phase current excitation parameterised globally within the project, for example:

$$\begin{aligned}&\text{IPeak*sin((pi*MachineRPM/1rpm*NumPoles/60}\\&\quad\text{*time} + (360-0)/360\text{*}2\text{*pi}) + \text{PhaseAdvance}) \qquad (2)\end{aligned}$$

By exciting the model via currents, the MMF and the flux produced by both the analytical and complex geometry windings will be the same for the given number of turns. This was tested and validated by measuring the torque produced by both a fully analytical model and the hybrid winding model.

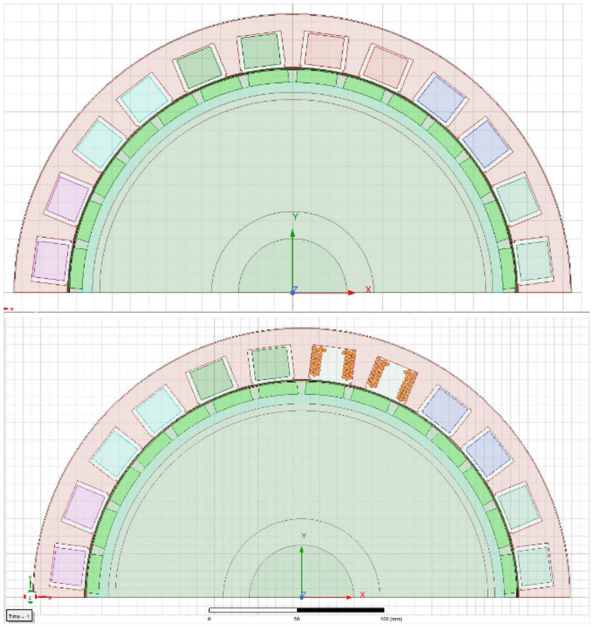

FIGURE 4. (Top) The analytical model, (Bottom) the hybrid model.

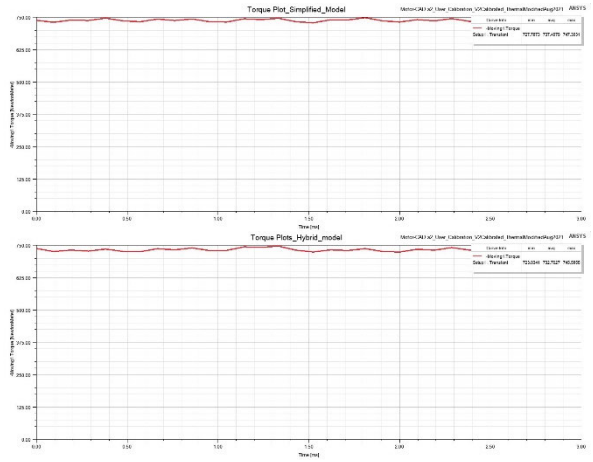

FIGURE 5. (Top) The torque produced by the analytical model, (Bottom) the torque produced by the hybrid model.

The only difference between both the fully analytical model and the hybrid winding model is the higher quality loss data enabled by representing the winding of interest as full geometry and loss data obtained from the full geometry winding was then superimposed upon all windings within the model to represent total machine losses, adjusted for symmetry within the model. Therefore, the performance of a given motor for a given winding design is:

$$\begin{aligned}&\textit{Total Losses}(W)\\&= ((I^2R + \text{Skin effect loss}\\&\quad + \text{proximity effect loss}\\&\quad + \text{Armature reaction loss)*total number o windings)}\\&\quad + \text{Magnet material loss} + \text{Stator Iron loss(Hysteresis}\\&\quad + \text{eddy current loss)} + \text{Rotor Iron loss.} \qquad (3)\end{aligned}$$

$$\text{Input Power (W)} = \sqrt{3} * \text{LineVoltage} * \text{I (rms)} * \text{PowerFactor} \quad (4)$$

Alternatively,

$$\textit{Input Power (W)} = \textit{Output Power} + \textit{Total Losses} \quad (5)$$

$$\text{Output Power (W)} = \text{Torque develped by the rotor} \; {}^{*}\text{rpm(in radians per second)} \quad (6)$$

$$\text{Efficiency}(\%) = \frac{\text{Output Power}}{\text{Input Power}} \quad (7)$$

Imposed model constraints will now be discussed in more detail.

- All conductors in the electromagnetic models are solid conductors. Bundled conductors were determined to be unfeasible due to the time to compute large numbers of conductors and increasing Finite element mesh complexity. The close proximity of conductor geometry would be impossible to render using metal additive manufacturing due to the inability to remove support structures between adjacent conductors.
- Conductor transposition was not included, as there is no way to represent transposition geometrically within a two-dimensional model. Whilst it would be possible to assume ideal transposition of conductors to minimise AC loss effects, there would be no way to render such complex geometry using additive manufacturing of metal, due to the inability to remove support structures between conductors, small conductor cross sections and geometry.
- Minimum and maximum conductor cross sections that a conductor can inhabit within the slot was limited to 1 mm^2 for the smallest cross section and 3 mm^2 for the largest. These values were ascertained by the largest slot area a conductor could inhabit if all conductors were the same cross-sectional area and the limitations of metal additive manufacturing precision, typically 0.5 mm^2. However, for the random placement strategy, conductors were allowed to surpass the 3 mm^2 limit, due to the nature of the strategy.
- Limiting the number of conductors comprising a winding to 48, helps limit *the number of possible variables to be altered*. With each conductor comprising of five variables, x-position, y-position, shape, scale and orientation, this amounts to 240 variables describing a windings structure and layout. Variable numbers rise sharply with increasing numbers of conductors. Additional variables were used to describe custom parameters within each of the layout strategies.

VIII. THERMAL MODELLING, UTILISING LUMPED PARAMETER THERMAL NETWORKS

The thermal model used was a lumped parameter network model produced in MotorCad. Both the concentrated and distributed winding models had their own unique thermal model setup. Lumped parameter thermal networks are widely used in the thermal analysis of electrical machines and can be preferential due to their reduced computational times [46]. The lumped parameter thermal networks were created within Ansys motorCAD utilising the benchmark winding layout illustrated in Figure 2. for both the concentrated and distributed winding topologies. The motor topologies were firstly simulated within the mechanical analysis tool within MotorCAD to characterise the behaviour of the motor. This data was then imported into the thermal analysis tool where thermal analysis took place. The LPTN's for both the concentrated and distributed winding layouts were then produced from the thermal behaviour. For complete analysis, the thermal and mechanical data was then applied to the electromagnetic simulation to ascertain a high precision loss model for the benchmark winding within MotorCAD for comparison against the hybrid Ansys Maxwell FEA equivalent models.

Lumped parameter thermal networks are often used to speed up the computation process of motor simulation by simplifying the thermal model complexity and use heat transfer theory to make estimations about the thermal behaviour of the system they represent [47], [48].

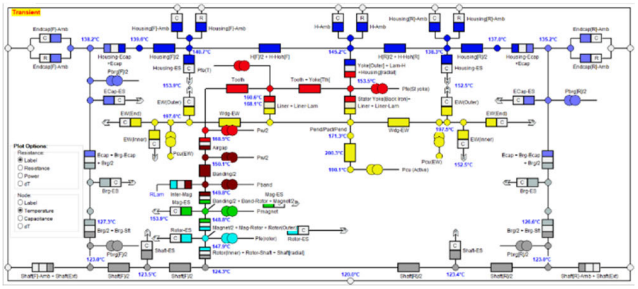

FIGURE 6. The concentrated winding machine lumped parameter network thermal model.

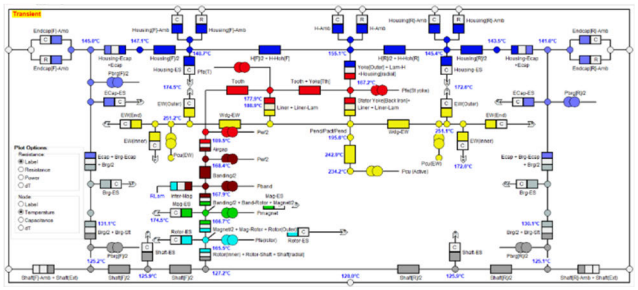

FIGURE 7. The distributed winding machine lumped parameter network thermal model.

Given the complexities of automating the entire optimisation process and attempting to keep simulation times as minimal as possible, the thermal models were static and not dynamic. The reasoning for the static thermal modelling was simple: a dynamic model would require an unpredictable number of simulations between the electromagnetic model and the dynamic thermal model before both models converged. This would ultimately bloat simulation time on a

per winding basis. The temperatures derived were from the benchmark thermal models of the concentrated and distributed windings. The temperatures for all materials within those models were then superimposed on to the materials of the equivalent models within hybrid Ansys Maxwell FEA model. These temperatures then determined material behaviour such as material resistivity for example.

TABLE 2. Thermal model parameters.

Parameters	Concentrated winding machine	Distributed winding machine
Winding temperature (°C)	190	234.2
Stator lamination temperature (°C)	153.5	167.2
Rotor lamination temperature (°C)	147.9	165.5
Magnet temperature (°C)	148.8	166.7
Rotor banding temperature (°C)	149.8	167.9
Shaft temperature (°C)	124.3	127.2
Housing temperature (°C)	20	20
Losses @ thermal model temps (W)	16228	21400
Efficiency @ thermal model temps (%)	89.862	81.838

Table 2 Shows lumped parameter thermal network parameters for the distributed and concentrated electric machines. These temperatures are for experimental purposes and may not be appropriate for every design or use case of electrical motors.

IX. THE NESTING PROBLEM

In order to best probe the design space, an automated optimisation process utilising MOGA is proposed, inspired by a mathematical problem called the ''packing problem'' or ''nesting problem''. These problems are defined as and belong to a class of cutting and packing problems which consist of allocating sets of regular and irregular shapes into typically rectangular containers or any shaped container whilst minimising waste space. The problem combines the combinational difficulty of cutting and packing whilst also being computationally challenging by enforcing geometric constraints such as non-overlaps of geometry and containment. This is exceptionally important if we wish to generate valid geometric layouts that can be simulated in FEA and translated to real-world geometry for manufacturing and testing.

Nesting problems have been addressed both in research and in real-world practical applications by heuristic, meta-heuristic and mathematical models. The packing problem arises in many different industrial and logistical applications and often involves or are involved directly in, more complex optimisation challenges [49]. The algorithm chosen to generate valid winding designs was the genetic algorithm. Genetic algorithms are used significantly within research to help optimise motor design parameters along with numerous other algorithms. They are stochastic search methods that take inspiration from biological processes such as evolution, survival of the fittest and genetics. Originally, genetic and evolutionary algorithms were developed to handle optimisation scenarios where no gradient information was available, such as binary, discrete search spaces and continuous variables. They are also good at handling large numbers of variables and failed states [50]. The overall algorithmic process is a multi-staged automated workflow and is shown in Figure 8, where it can be seen that there are prior steps that are taken before passing variable data to the multi-objective genetic algorithm. These are pre-processing steps which include sensitivity analysis.

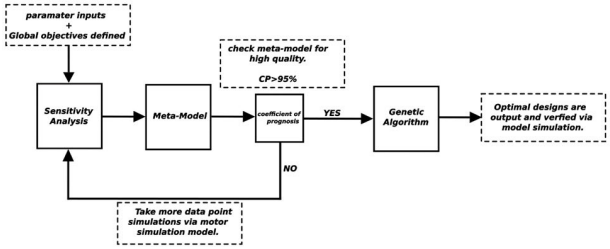

FIGURE 8. The algorithmic process.

X. SENSITIVITY ANALYSIS

Sensitivity analysis is the study of how the output of a model can be evaluated, either qualitatively or quantitatively with regards to varying sources of input [51]. Variance methods are used to quantify the effects of a random input variable on the output variance of the model. Variance based sensitivity analysis is used as an optimisation pre-processing tool. It represents continuous optimisation variables by uniform distributions, without variable interactions. Sensitivity analysis is used to quantify the contribution of an optimisation variable to the potential improvement of a model's response. It quantifies the contribution with respect to defined variable ranges [52]. However, typically sensitivity analysis requires large amounts of data, computation and simulation effort.

XI. LATIN HYPERCUBE SAMPLING

Sampling methods are used as a basis for constructing the surrogate model or in this case the meta-model of optimal prognosis. Latin Hypercube sampling stratifies the variables by randomly sampling from each of the stratified parameter variables, with a sample taken from each interval. The number of sampling points taken is equal to the number of levels. Latin Hypercube sampling has benefits such as sampling efficiency and reduced runtime iterations by enabling more efficient space-filling [41], [53]. Figure 10 shows a comparison between latin hypercube sampling and other sampling methods

XII. META-MODELLING – THE META-MODEL OF OPTIMAL PROGNOSIS

The Meta-model of optimal prognosis (MOP) is used as a mathematical surrogate model mapping the relationship between the input and output variables and the various relationships that comprise them. Common models used, are polynomial regression, response surface methodology (RSM), RBF/EBF Neural Network, support vector machines (SVM) and kriging.

MOP is capable of fitting complex response relationships with good robustness and strong practicability. With suffi-

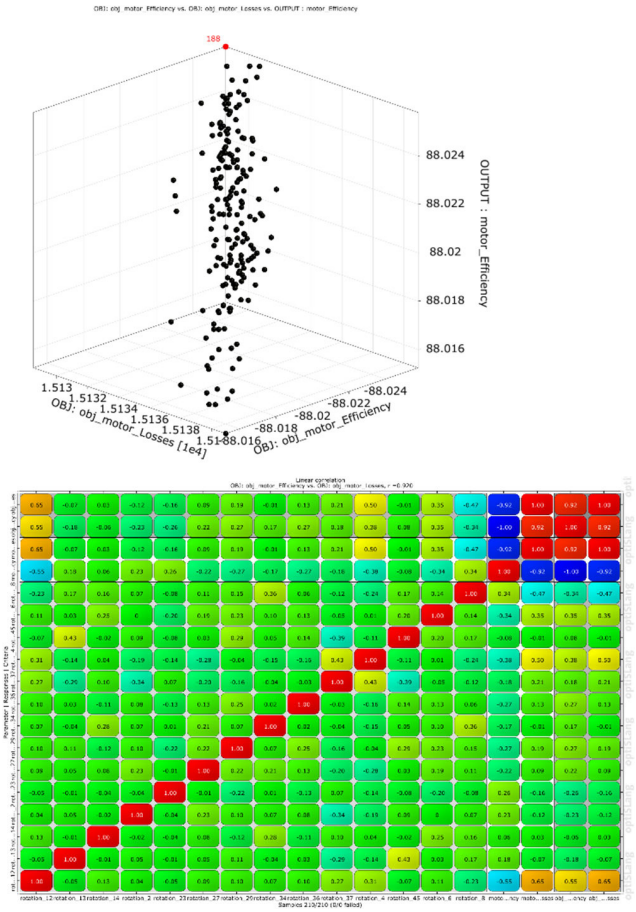

FIGURE 9. (Top) An example of a pareto front of possible designs and (Bottom), the linear correlation matrix, visualising the relationship between input parameters and output responses.

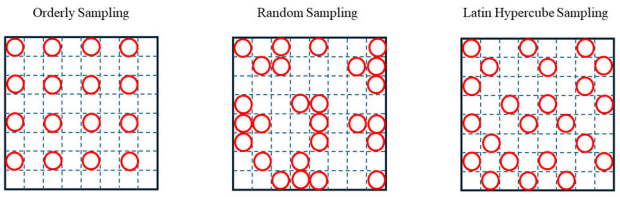

FIGURE 10. Latin hypercube sampling compared to other sampling strategies.

cient accuracy, the MOP is capable of representing complex models such as the hybrid finite element analysis PMSM winding model presented in this paper. The MOP improves the optimisation time especially with large parameter sets and complex functional relationships. However, the response surface is not guaranteed to pass through all sample points and so a small error remains. It is necessary therefore to analyse the fitting accuracy of the MOP compared to the original model it represents, therefore the Coefficient of Optimal Prognosis (COP) is used as a measure of meta-model accuracy. The COP is a cross-validation, which is an objective and quantitative evaluation of the predication quality of the MOP. Figure 11 shows a comparison between the response data and the FEA PMSM model values.

The higher the COP achieved the greater the quality and accuracy of the meta-model compared to the model it represents. A COP of >0.7 is considered good fitting, however for the research presented in this paper and the complex relationships that are modelled, a COP of > 0.95 was considered.

Whilst meta-modelling and sensitivity analysis is still computationally intensive, involving large data sets (in this case $\sim$300-500 samples/simulations per experiment stage), it allows the surrogate model to be improved by removing unimportant variables and reducing variable ranges within the model. This is important as the predictive quality of a meta-model through sensitivity analysis rises as the number of variables decreases [54].

Meta-modelling allows for the rapid evaluation of design trade-offs and is a common tactic used in motor design [30].

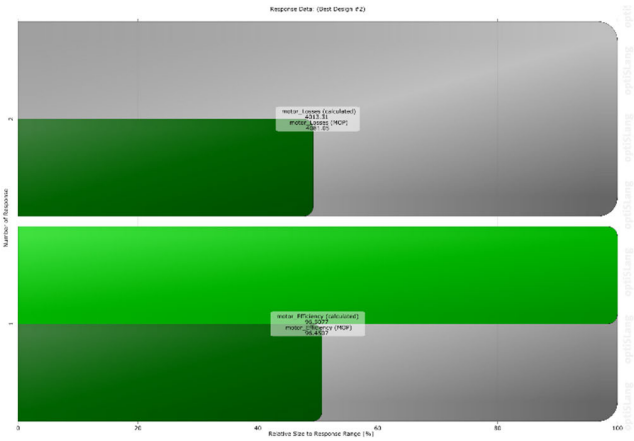

FIGURE 11. The response data, illustrating the accuracy of the MOP against the calculated model values for efficiency and losses.

XIII. AUTOMATION OF THE OPTIMIZATION PROCESS

Automation played a crucial role in getting the entire simulation process to work. It was necessary as tens of thousands of custom winding simulations with entirely new winding geometries would need to be processed. Python was utilised as it was incredibly flexible and has a wealth of powerful API's. Ansys Optislang where the automated optimisation process was constructed, is capable of interacting with, and loading Python scripts. Variable values can be inserted into a Python script directly from Optislang itself, with prior appropriate setup. A large number of Python language-based tools were scripted to handle geometric construction and drawing of the windings derived from the parameters set by Optislang. Windings were validated and checked for boundary conditions and overlapping of geometry. An automation file was then generated from winding data. The automation file contained instructions in the visual basic language which was processed and run by the Windows operating system. The automation instructions opened Ansys Maxwell, loaded the hybrid FEA model with the appropriate empty slots, and then proceeded to draw the

winding geometry and setup up all the appropriate parameters to run the simulation.

Output data from the simulation was then placed into a uniquely identified folder accompanied by data such as screenshots, excel files containing winding and loss data, torque values and a copy of the processed simulation data for later use and reference. The python script would then read the accompanying data in the appropriate folder and present the values back to the optimisation process illustrated in Figure 12.

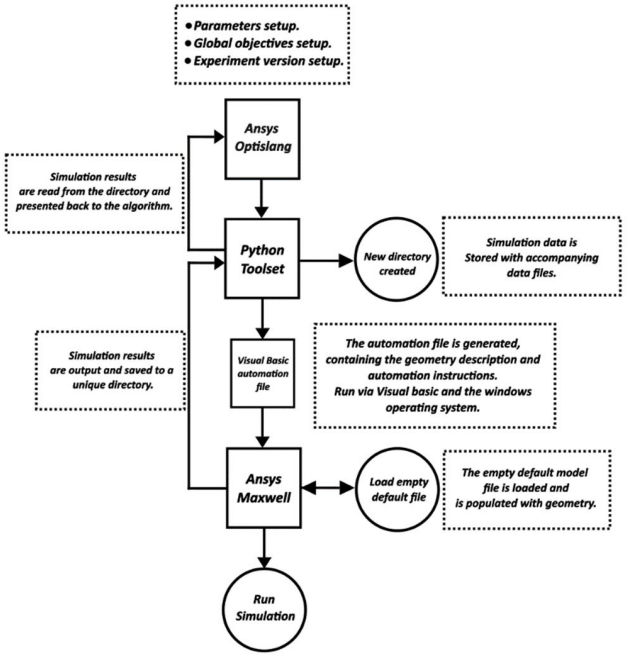

FIGURE 12. An illustration of the entire automation process for simulating winding designs generated by the algorithm.

XIV. EXPERIMENTAL CONDUCTOR PLACEMENT STRATEGIES

Four placement strategies were devised for both the concentrated winding and distributed winding layout: orderly conductor placement, layered conductor placement, randomised conductor placement and clustered conductor placement. The orderly conductor placement strategy arranged the conductors in an orderly fashion, where conductors were equidistant and uniformly placed within the slot. Each conductor had a defined and pre-determined area for which they could move, scale, change shape and orient themselves within. The layered placement strategy built upon the orderly strategy. The slot was divided into sub domains that could grow or shrink in height. The randomised conductor placement strategy utilised an adaption of the fractal random algorithm by authors Shier and Bourke [55]. The unique placement algorithm attempts to solve the packing problem with the random placement, shape, size and orientation of conductors within the slot. A purely randomised placement is exceptionally time consuming and is not guaranteed to solve. Therefore, a fractal randomness is utilised, where every n^{th} conductor is slightly smaller than the last. The difference in the conductor scales between every n^{th} conductor is dictated by values of C and N.

$$S(c, N) = \sum_{i=0}^{\infty} 1/(i+N)^c \tag{8}$$

The Hurwitz zeta function is an ever-decreasing exponential function, whose values of C and N were pre-computed using the algorithmic process detailed previously in Figure 8. Lastly, the clustered conductor placement strategy, placed conductors within a volume that could be moved around the available slot space. This arrangement was loosely inspired by bundled conductors. Each of the experiments were ran four times, with each starting stage consisting of a seed shape, either square, circle, triangle or hexagon. The experiments were separated into stages, each stage representing one of the degrees of freedom such as conductor position or shape. The end product of each stage generated by the optimisation process was then used to seed the next stage illustrated in Figure 13. This was done for several reasons, which included, a reduction in complexity, a reduction in the number of variables being altered, improved insight into the process, and a thorough exploration of the design space. Example winding outputs are illustrated in Figure 14.

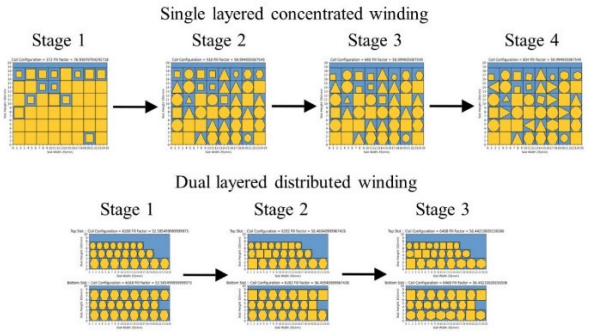

FIGURE 13. The optimisation process example stages.

XV. RESULTS AND DISCUSSION

In total 46 winding designs were generated, with 24 concentrated single layered designs and 22 distributed dual layered designs. Winding designs were assigned a number, which identifies that design. The number represented the current simulation iteration that the design was simulated. Henceforth, winding designs will be referred to as #7777 for example, in this paper.

To verify the two-dimensional model results and the end winding losses, two high precision three-dimensional models were created from windings #9354 and #2043 in table 3 for comparison. Both winding models were modelled on a per conductor basis and included the end winding sections. The assumption was that the end winding behaviour was primarily DC loss and as such, the end windings were modelled to be as short as possible. If the machine was sufficiently high in

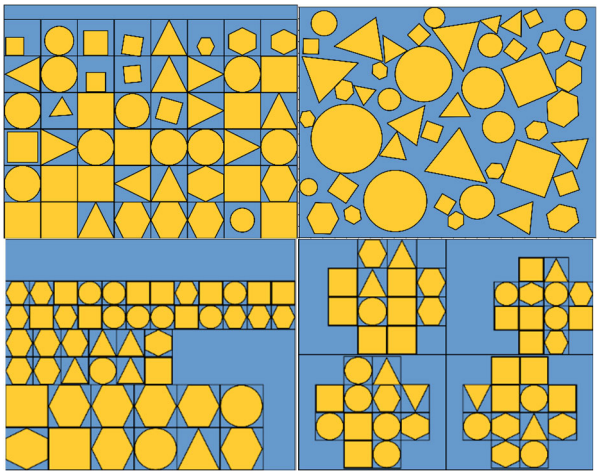

FIGURE 14. Top left, orderly placement, top right, random placement, bottom left, layered placement and bottom right, clustered placement.

operating speed, for example 12,000 RPM, or operational frequency greater than 1000 Hz, then AC effects such as proximity effects from the windings interacting with stator lamination ends would occur, requiring the end windings to be extended in length to avoid this interaction at the expense of additional DC loss [8].

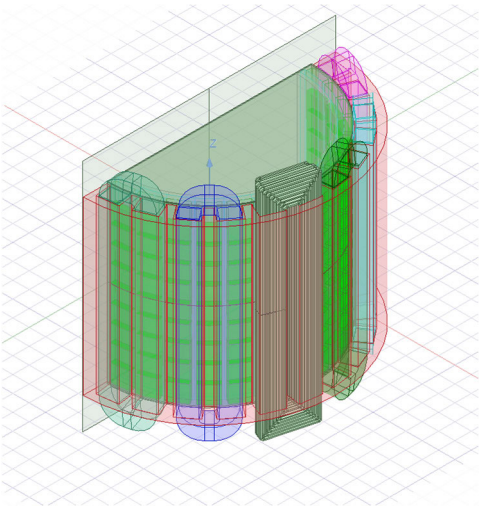

FIGURE 15. The 3D high precision simulation.

It was found that the losses observed in the high precision simulations agreed with the two-dimensional assumptions for end winding behaviour. The high precision simulation included an additional ∼28% more DC losses when compared to the two-dimensional model's loss values for #2043 and #9354. This coincides with the additional 28% winding mass making up the end windings, confirming that the end winding loss behaviour is primarily DC losses.

The simulation results will be validated experimentally in a future paper via a motorette sub-assembly. One of the most performant winding designs, #9354, was chosen

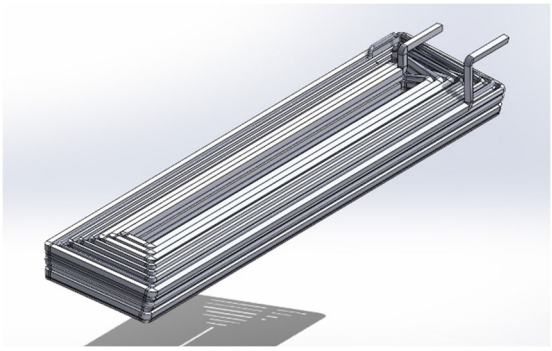

FIGURE 16. The 3D model of the concentrated winding.

TABLE 3. 3D simulation results.

Winding design no.	2D winding loss (W)	3D winding loss (W)
2043	4737.381	6063.848
9354	3967.092	5239.739

TABLE 4. Concentrated winding data.

Concentrated windings	Winding number	Efficiency (%)	Fill factor (%)	Losses (W)	Copper usage per winding (kg)
Orderly placement	834	94.552	58.994	6395.111	1.371
	1211	95.359	68.128	5395.708	1.583
	1560	94.953	66.850	5890.950	4.554
	2043	95.901	63.256	4737.381	1.470
Random placement	3547	87.627	51.001	15644.435	1.185
	3952	87.674	56.324	15572.195	1.309
	4712	87.422	47.732	15950.836	1.109
	5172	87.910	51.608	15236.571	1.199
Layered placement (4 layers)	5943	93.182	49.037	8128.361	1.140
	6523	93.872	53.586	7239.092	1.246
	6741	93.912	55.471	7179.393	1.289
	7679	94.498	52.764	6458.019	1.226
Layered placement (6 layers)	8032	97.168	64.802	3234.438	1.506
	8504	95.978	66.466	4645.141	1.545
	8937	96.101	65.632	4497.425	1.526
	9354	96.546	60.326	3967.091	1.402
Clustered placement (4 clusters)	9723	95.258	48.986	5523.735	1.139
	10337	92.444	40.094	9074.078	0.932
	10876	94.007	45.939	7074.692	1.068
	11340	93.423	39.423	7812.141	0.919
Clustered placement (6 clusters)	11811	92.758	34.381	8677.970	0.799
	12016	88.835	28.193	13972.934	0.655
	12500	88.154	27.756	14937.155	0.645
	13178	89.151	26.289	13534.081	0.611

for manufacture based on its suitability for additive manufacturing, determined by a Simufact additive simulation. A concentrated winding was chosen due to the ease of manufacturing the winding layout compared to a distributed winding, which consists of two layers and larger, more complex end winding structures. The stator piece could also be significantly smaller compared to the stator piece required to house a distributed winding, thereby saving on manufacturing cost and complexity.

The most performant winding designs were 6 to 7 percent more efficient when compared to the original benchmark winding layout produced in MotorCad. Winding designs #8032 and #9354 were the most performant. Whilst there are additional fill factor gains of around 30%, it was observed that fill factor increases are variable on a per winding basis as seen in Figure 17. All of the most performant winding designs conform to the layered placement strategy (6 layers), holding true for both concentrated and distributed

TABLE 5. Distributed winding data.

Distributed windings	Winding number	Efficiency (%)	Fill factor (%)	Losses (W)	Copper usage per winding (kg)
Orderly placement	534	83.901	44.767	19285.682	1.873
	1109	85.752	64.403	16663.325	2.695
	1530	85.299	50.978	17314.636	2.133
	2138	87.043	54.103	14947.232	2.264
Random placement	2179	80.531	41.479	24343.431	1.735
	2334	81.041	46.409	23416.067	1.942
	2409	79.386	39.519	25998.047	1.653
	2538	80.613	42.025	24218.184	1.758
Layered placement (4 layers)	3192	87.228	56.781	15122.020	2.376
	3803	86.612	57.645	15959.668	2.412
	4515	86.397	44.678	16347.248	1.869
	4908	87.698	54.929	14514.716	2.298
Layered placement (6 layers)	5347	88.281	66.163	13341.904	2.768
	5735	87.999	64.080	13709.625	2.681
	6031	87.573	64.824	14240.872	2.712
	6468	88.333	56.442	13394.104	2.361
Clustered placement (4 clusters)	7003	86.923	46.919	15158.458	1.963
	7516	85.563	44.373	17004.059	1.857
	7950	85.327	42.882	17327.528	1.794
	8574	85.521	42.882	17062.608	1.794
Clustered placement (6 clusters)	9115	83.738	32.761	19554.034	1.371
	9722	80.204	27.482	24895.356	1.149

winding configurations. Similarly, to the concentrated winding designs, the fill factors for the distributed windings are also variable per design. It was observed that winding #6468 utilises less fill factor (56.44% compared to 66.16%) than winding #5347 whilst remaining narrowly more efficient.

In terms of the worst performing designs for both concentrated and distributed winding layouts, almost unanimously belong to the random placement strategy for both sets of data in tables 4 and 5. Interestingly, even with additional fill factor of around 26.32% gained by winding design #3952 over the default windings design of 30% fill factor, #3952 is unable to match the benchmark windings efficiency of 90%, with winding #3952 only able to achieve an efficiency of 87.67%. This behaviour is mirrored in the distributed winding designs, where winding design #2334, a random placement winding with an additional fill factor of 16.4% over the default winding, is unable to match the distributed default winding efficiency.

The effect that randomness has on the performance of a winding design continues to be validated with the clustered placement strategy. The clustered layouts containing 6 clusters had random conductor positions chosen within their bounding volumes. The most performant six-clustered concentrated winding design is #11811 which has a fill factor of 34.88% and is only able to attain an efficiency of 92.75%. The worst performing six clustered concentrated winding design is #12500 which has an efficiency of 88.15% at a fill factor 27.75%, just 2% less fill factor that the benchmark winding. The result is mirrored in the six clustered distributed winding designs in table 5 where winding #9115 is only able to obtain an efficiency of 83.73% with a fill factor of 32.76%. The worst six clustered winding design is #9722 whose efficiency is the second poorest of the entire dataset at 80.20% with a fill factor just 2.5% less than the benchmark distributed winding design. Therefore, it can be noted that any kind of randomness within a winding design has a meaningful and sometimes detrimental impact on a winding's performance. A similar observation was seen by Stoyanov and Selema, where it shown that the random allocation of conductors in the slot can lead to excessive losses and poor fill factor [56], [57]. Fill factor and its utilisation is also a complex relationship when it comes to winding design. Typically fill factor is seen as a "good" metric for low loss winding performance. However, this ignores AC effects such as skin and proximity effects, along with armature reaction. In modern motor design, the conductor profile, arrangement and lay in stator have become an ever-increasingly important consideration [10]. Figure 17 illustrates the relationship of fill factor versus efficiency for both concentrated and distributed winding designs.

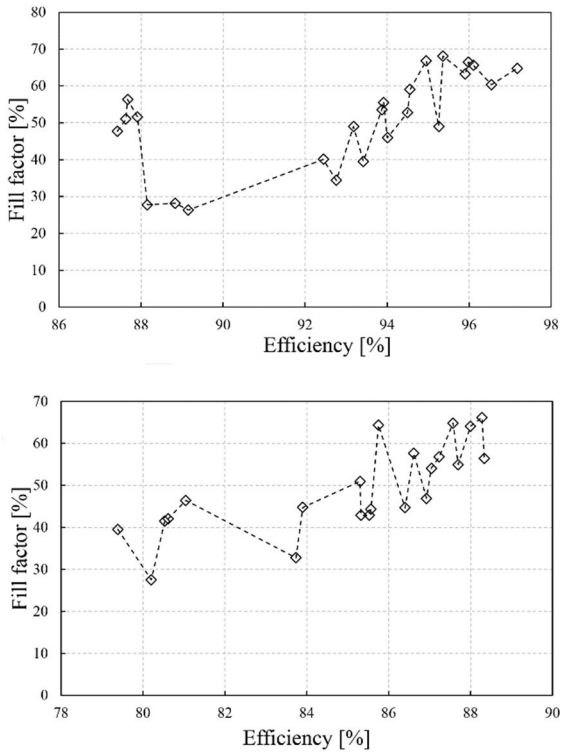

FIGURE 17. (Top) Fill factor versus efficiency for concentrated winding designs, (Bottom) Fill factor versus efficiency for distributed winding designs.

Whilst there is a broad trend in both graphs in Figure 17 that increasing fill factor corelates with increasing motor efficiency, the trend is not completely linear. It can be seen that certain winding designs are able to minimise copper winding mass usage whilst simultaneously achieving higher performance than some of the previous winding designs. For example, Table 4 shows that winding #9354 with an efficiency of 96.54% utilises 60.32% fill factor and has a winding mass of around 1.402 kg. Consequently, the prior best performing winding #8937, has an efficiency of 96.10% and a fill factor of 65.63%, with a winding mass of 1.525 kg. When calculating the differences in mass savings between both windings, it can be seen that, with 12 windings situated

in the stator, winding #9354 saves around 1.48 kg of copper, compared to winding #8937.

A more dramatic example is windings #9723 and #1560. Winding #9723 has superior efficiency at 95.25% compared to winding #1560 at 94.95% efficiency. The copper savings however are around 4.983 kg. Similar savings can be seen in the distributed winding graph in Figure 17 and Table 5 where winding #6468, the highest performing distributed design, utilises 56.44% fill factor, outperforming winding #5347 in efficiency, whilst using around 9.72% less fill factor. This equates theoretically to a saving of roughly 4.88 kg of winding copper mass. These results illustrate some potential opportunities afforded by additive manufacturing to decrease stator copper winding mass whilst maintaining or possibly gaining performance. This could help save material cost, increase motor power densities and make the device smaller and more compact.

Windings designed for additive manufacturing could potentially offer benefits in aerospace, automotive, automotive sports such as formula-E and other applications. All winding mass approximations include the end winding mass. The winding designs that were the most performant were created with the layered strategy. These designs shared a common trend in terms of conductor placement, even though each final design was evolved separately.

Note, spaces in the winding seen in Figure 18, denote the top and bottom sections respectively. This spacing does not occur within the slot.

The predominant features that make up the designs are typically larger conductors situated at the bottom of the slot, with medium to smaller conductors placed centrally. Another prominent feature is the use of smaller conductors placed at the top of the slot, resulting in a tier like layered structure. Large conductors with more fill factor are used to combat DC losses. Square conductors are prominent in a few of the designs, especially #8032 and #6468. This is due to square conductor's large copper surface area, compact winding structure and space saving capabilities. Square conductors have also been shown to have superior electrical and thermal performance at lower frequencies [57].

Another feature is the use of different shape utilisation and position. Different shapes have differing cross-sectional areas when compared to square conductors. The use of combinations of circles, hexagons and triangles may be deployed in order to mitigate AC losses such as proximity effects encountered by the winding design. Changing conductor size, shape, orientation and position within the slot may aid in increasing the distance between conductor facets, therefore decreasing the volume of a conductor exposed to an external field [58].

In 1924 Butterworth [59], showed that the proximity effect decreases with increasing distance. This is due to the magnetic field B, decreasing in magnitude with increasing distance. The increased distance between conductor centroids means the induced eddy currents experienced by the surrounding conductors also decreases. The decreased eddy currents therefore give way to a more uniform current density within the affected volume of the conductor. Since the power loss observed is equal to the square of the current density (9), a more uniform current density results in less power loss being observed in the affected conductor. The interplay between conductor shape, size, orientation and position help to balance the DC and the AC losses being incurred by the winding design. Proximity effects are assumed to be the dominant AC loss effect, as the skin depth calculated for the machine operating at 1500 RPM was around 3.5mm. Thus, only conductors larger than 3.5mm in height would encounter skin effect losses.

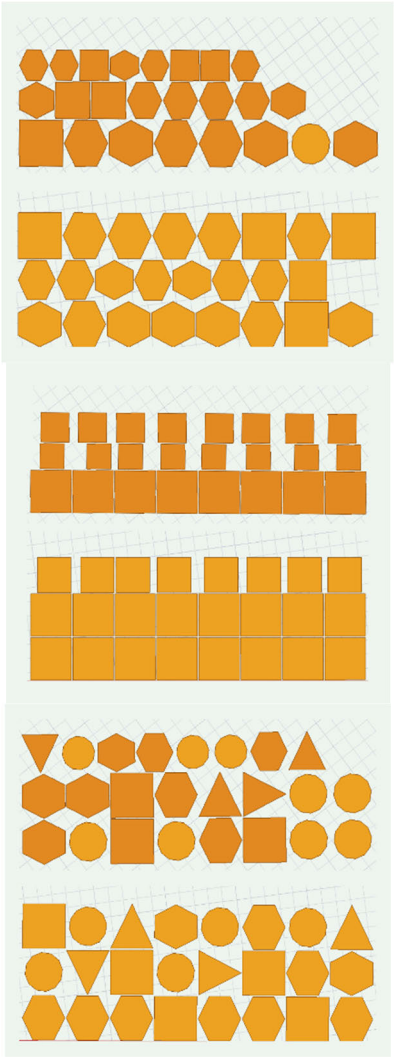

FIGURE 18. Distributed winding designs, from the top, #6468, #5347 and #5735.

$$P_{AC} = \frac{1}{\sigma} \int_{Volume} J^2.dV \tag{9}$$

A layer of small conductors at the top of the winding have been placed in many of the designs. This structure has been placed strategically by the algorithm, to avoid potential losses

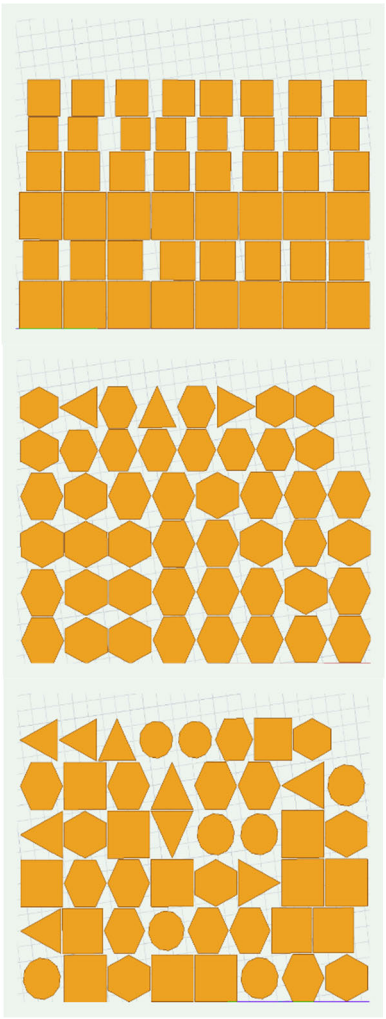

FIGURE 19. Concentrated winding designs, from the top, #8032, #9354 and #8937.

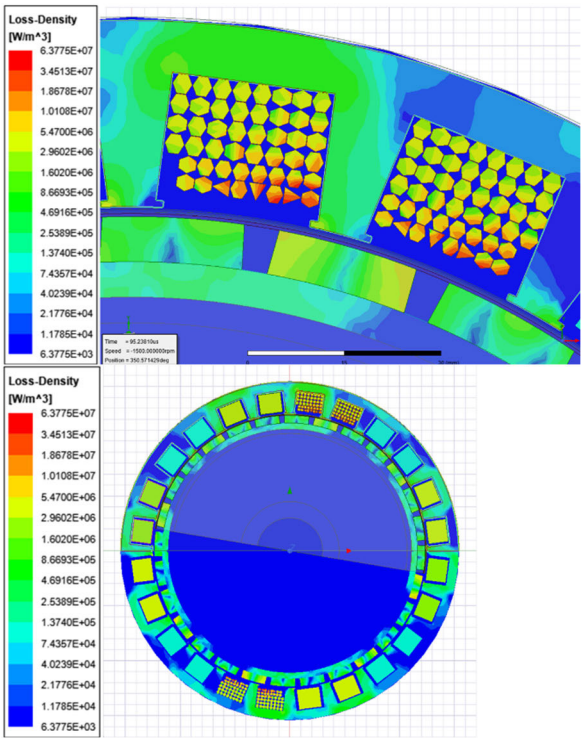

FIGURE 20. (Top) The loss density exhibited by the conductors comprising winding design #9354 and (Bottom) The CEFEA concept illustrating the symmetry used within the PMSM Maxwell model.

produced by the interaction of the winding with the armature field. A similar strategy was shown with a winding consisting of hollow additively manufactured conductors, where solid smaller conductors were placed at the top of the winding. It was found that solid small conductors at the top of the slot were better at mitigating armature field losses compared to hollow conductors [24]. The inclusion of tooth tips also helps aid in minimising flux leakage from the armature field. The tooth tips provide more optimal tangential routes for flux to travel to the stator teeth. This results in better utilisation of permanent magnet material and higher air gap flux [60].

Figures 21 and 22 show that low speed losses are minimised and as speed increases, the losses increase sharply for the concentrated windings and more steadily for the distributed windings. Comparing the random placement winding designs in Figure 21 and Figure 22 the low speed losses are substantial, whereas the loss increase with increasing speed is more linear. This may be due to the differing ways that windings have been structured. The random winding placement contains many small conductors with large spaces between them disregarding armature field loss mitigation. The random placement strategies differing conductor cross sectional areas lead to increased DC loss and ohmic losses, especially at lower speeds. Whereas the most performant layered windings are efficient at lower speeds. The predominant losses are DC loss with armature reaction and proximity losses making the AC losses which scale with motor speed. The windings are heavily biased towards DC losses and the optimisation point of 1500 RPM. Note that there are small differences in the peak performance in Figures 21 and 22 between the windings suggesting the layouts of the windings do have an impact on the AC losses incurred at those motor speeds.

Comparing the data sets by placement strategy, it can be observed that the mean efficiency was achieved by the 6 layered conductor placement strategy for both concentrated and distributed winding designs, which agrees with the fact that both the most performant winding designs #8032 and #9354 both belonged to that design strategy for conductor placement. The lowest mean efficiency was observed in the random placement strategy, which consequently results in the largest mean losses. This shows that conductor placement is pivotal to reducing losses and increasing overall motor efficiency, when it comes to winding design. This is reflected in the median data set graphs.

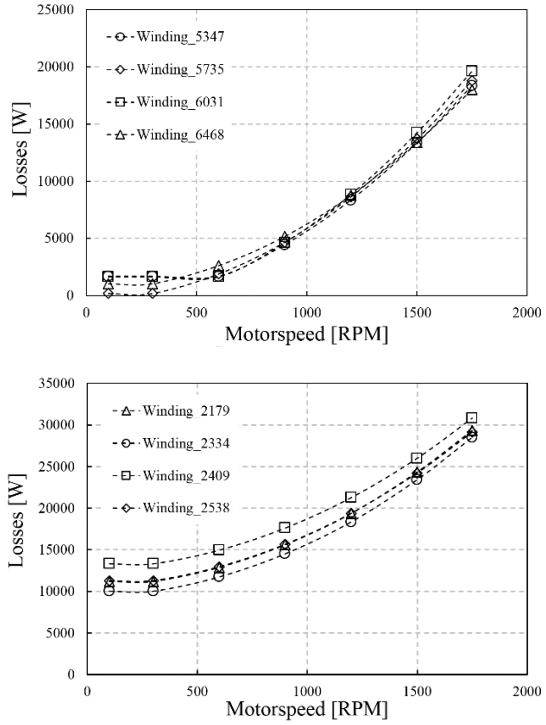

FIGURE 21. (Top) Distributed layered winding loss versus motor speed graph and (Bottom) Distributed random winding loss versus motor speed graph.

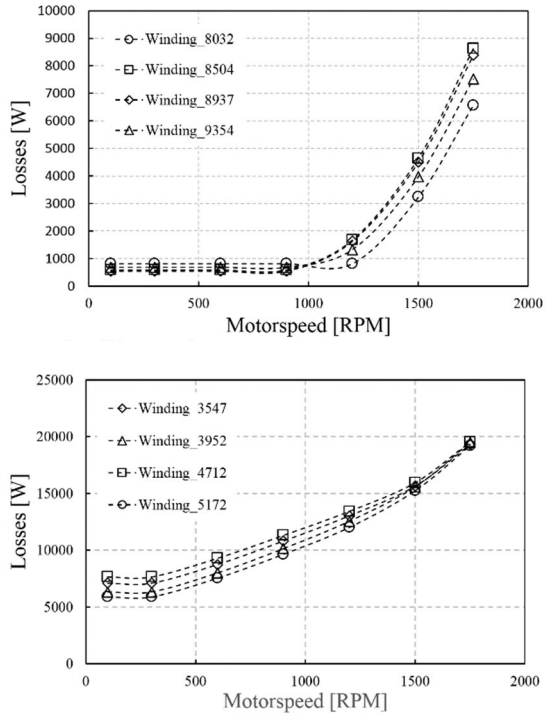

FIGURE 22. (Top) Concentrated layered winding loss versus motor speed graph and (Bottom) Concentrated random winding loss versus motor speed graph.

The standard deviation is high for both efficiency and losses graphs for the clustered strategy using 6 clusters. This may be due to the use of random placement of conductors within each cluster, but also the movement of clusters within the slot and the lack of fill factor. The lowest standard deviation for both efficiency and losses was observed for the layered strategy using 6 layers indicating consistency with the mean values for that respective strategy.

The distributed windings appear to show more deviations in the data set for efficiency, possibly due to the fact that there was a dual winding placement per slot affecting the ability for the algorithm to place conductors more strategically. The variance also shows that the clustered placement strategy with more clusters varies significantly for both concentrated and distributed windings, due to the random placement of the conductors within the cluster and the limited fill factor utilisation thereby increasing losses and varying the results more dramatically compared to mean values. The graphs for the mean, median, standard deviation and variance by objective function can be seen in Figure 23.

XVI. FUTURE POSSIBILITIES AND USE CASES

These results show that there may be a way to tailor a windings loss profile based on the ratios of small, medium and large conductors and their configuration within the slot. Utilising the same process detailed in this paper on a predesigned winding, a ratio of small, medium and large conductors could be chosen to tailor windings for a specific application. With further innovation in the additive manufacturing of metal, it may be possible to render small, bundled conductors, with paralleled conductors or idealised trans positioning to offset proximity and skin-effects, whilst retaining as much fill factor as possible. Such features have been demonstrated in larger, flat rectangular windings by Acquaviva et al. [27].

A feature that could be integrated is the inclusion of hollow windings in specific conductors. Larger cross-sectional conductors could be strategically chosen within a winding design to include a coolant pathway. Typically, hollow conductors are difficult to bend with small radii, however additive manufacturing could alleviate such manufacturing difficulties. It was found by Wu et al. [24] that the inclusion of selected hollow conductors within a winding allowed for maintaining fill factor whilst minimising AC loss through the use of a thermal management system. It was shown that a ratio of (50:50) of solid and hollow windings was the most optimal for heat extraction from the winding whilst remaining comparatively performant to an all-solid winding. The inclusion of a fully dynamic thermal model could potentially allow the optimisation process described in this paper to selectively choose the most optimal conductors to use as hollow conductors for heat extraction directly from the winding. Such a winding geometry would only be possible through additive manufacturing.

A potential example of using the process described in this paper could be in the application of motorsport such

FIGURE 23. Statistical analysis graphs for the objective functions of efficiency and losses. The graphs for mean, median, standard deviation and variance by objective function are shown.

as formula-E, where a vehicles performance on a specific track could influence the design of the windings being utilised in the traction system. By taking into consideration the ratio of DC and AC losses incurred on a particular circuit, the varying high speed and low speed sections could influence the winding structure. The data collected along with an optimisation study could potentially inform the best winding layout by inferring the ratios of large, medium and small conductors, their position, shape and orientation. This information would help inform the best winding layout along with desired loss characteristics over a specific speed range for a desired parameter set. Such customised high-performance windings would only be possible, utilising the design freedoms afforded by additive manufacturing and an algorithmic optimisation process such as the one detailed in this paper.

The optimisation of windings could help achieve better drive cycles for traction motors within the automotive space for example WLTP-3, C-WTVC and NEDC for example. Operational areas of a motor are highly dependent on the environment, such as urban, rural or highway driving scenarios. For automotive applications electric motors are typically optimised for material cost minimisation, which affects weight, volume and operational losses (efficiency). They also require knowledge of loss energy within an automotive drive cycle [43].

Another area that can benefit greatly from the optimisation of windings is the aerospace industry where the electrification of aerospace is a specifically challenging area, involving strict motor parameters set by the ASCEND project [43]. The ASCEND project performance characteristics are highly demanding of the motors required, for example, a maximum specific power of 20 kW/kg (motor active SP) should be attained, and the motor should run with high efficiency at a continuous operation of 5000 RPM for one minute (take off). The challenge, however, is that there are two unique operational points to be considered, base speed and peak power. This is a dichotomy since the Rac/Rdc is uniquely different for each operating point, with both AC and DC loss mechanisms being in stark contrast to one another. However, with optimisation processes discussed in this paper, a number of winding designs could be collated that are derived at each operating point, and then further optimisation could be done, using the same process to ascertain a final winding design that could best fit the operating scenarios whilst minimising the trade-offs as much as possible. Therefore, complex winding designs such as those detailed in this paper could help achieve windings that have less mass, as illustrated in the findings but also help achieve less losses making the winding more efficient and the motor topology more able to meet the demanding requirements of aerospace projects like ASCEND.

The most performant winding designs achieved with the optimisation process described within this paper were concentrated windings #8032 and #9354, efficiencies achieved being 97.168% and 96.546% respectively. These efficiencies were achieved at a single operating point of 1500 RPM whilst manipulating only the winding structure and no other part of the motor topology, for example magnetic material utilisation, stator topology, rotor topology or material properties.

Many papers discuss the optimisation of electrical motors from many different perspectives, not limiting their optimisation pathways solely to winding structures. For example, in [42] by Wei et al., discusses the optimisation of energy distribution and topology parameters of a PMSM motor over the C-WTVC drive cycle consisting of 10 operational points. The resultant was an efficiency increase of 97.01% to 97.40%.

In Mirhaki et al. [61], a wound field synchronous motor winding was optimised as an alternative to PMSM for electric vehicle applications. The process described is similar in its utilisation of GA, MotorCAD, and Maxwell models to optimise the rotor windings and number of poles over a 10 point operating cycle. The achieved efficiency was 95%. Al-Quarni and EL-Refaie [62], describe the optimisation of concentrated additively manufactured AlSi10Mg hybrid hollow-stranded windings for use in electric aircraft, constrained by the ASCEND project requirements for specific power of 20 kW/kg. It consists of two operating point optimisation with peak power efficiency achieved being 92.9% and continuous power efficiency of 94.2%. The solid stranded windings placed at the top of the slot help alleviate armature reaction losses.

Tripathy et al. [36] use particle swarm optimisation and genetic algorithms to increase the efficiency of a squirrel cage induction machine by manipulating numerous geometric and material factors in a global manipulation of motor topology. The authors were able to raise the motors efficiency from 84.147% to 94.02%, however neglected winding optimisation. Celik et al. optimise the use of magnetic material in a PMSM motor designed for airborne wind energy concept systems. The optimisation process utilises an analytical motor model with thermal and mechanical constraints. The motor topology was optimised along with the minimisation of cobalt-iron was optimised to minimise cost and weight due to the fact that the machine would be airborne. The authors achieved a power density of 1.8 kW/kg with an efficiency of 96%. Simpson et al. [2] utilises the additive manufacturing of AlSi10Mg to produce concentrated windings containing a hybrid strand topology to minimise AC loss by parallelising turns near the top of the slot with sub-conductors. The result was a reduction in losses by 40% compared to a baseline design.

Whilst there are numerous pathways to optimise electric motors, winding optimisation may yield the greatest results as the windings are an active component and are the site of substantial losses within the machine. It is also noted that substantial weight savings can be gained by optimising the winding structure thereby reducing material cost and increasing power density, whilst potentially making the device smaller and more compact. Materials and manufacturing

costs are substantial factors in mass production scenarios. Whilst other research details sweeping topology wide and material changes to achieve optimisation goals, this paper details the effect of concentrating heavily on winding structure optimisation and conductor placement in achieving motor optimisation goals.

XVII. CONCLUSION

This paper presents an algorithmic approach to electric motor winding design in order to find the most optimal conductor placement to minimise losses associated with low fill factor, armature reaction and AC losses. The windings designed were optimised for a specific operating point of 1500 RPM at elevated temperatures. The resulting winding designs have been created based on 240 design variables describing the winding, tens of thousands of FEA simulation data and hundreds of thousands of algorithmic iterations. In this case study, it was found that the process yielded winding designs that were approximately 6-7% more efficient at operating temperature when compared to a benchmark winding layout. It was also found that weight savings could be made on a per design basis. This could enable a motor to potentially be more efficient and power dense by utilising an optimised additively manufactured winding that saves on material whilst maximising overall motor efficiency.

Further algorithmic optimisation processes were suggested to include the use of hollow windings for thermal management systems integration and shaping the ratios of small and large conductors comprising the winding to make the winding more efficient over a greater range of operating frequencies. The research presented focusses on solid windings that will be manufactured using Direct Metal Laser Sintering. Windings have been manufactured in AL10mgSi and Steel 316L and will be tested and validated against experimentally with a motorette sub-assembly. Additively manufactured windings whose geometries are optimised using algorithmic processes presents potential opportunities in improvement of electrical machines output performance. This paper presents and details the foundations for winding design and optimisation processes that have been developed for PMSM machines but are not solely limited to such topologies. The design tools and winding layouts presented here offer the ability to take advantage of the geometric freedom offered by present and potential future innovations in metal additive manufacturing technology.

REFERENCES

[1] S. Sakunthala, R. Kiranmayi, and P. N. Mandadi, "A study on industrial motor drives: Comparison and applications of PMSM and BLDC motor drives," in *Proc. Int. Conf. Energy, Commun., Data Anal. Soft Comput. (ICECDS)*, Kalikiri, India, Aug. 2017, pp. 537–540.

[2] N. Simpson, J. Jung, A. Helm, and P. Mellor, "Additive manufacturing of a conformal hybrid-strand concentrated winding topology for minimal AC loss in electrical machines," in *Proc. IEEE Energy Convers. Congr. Expo. (ECCE)*, Vancouver, BC, Canada, Oct. 2021, pp. 3844–3851.

[3] A. Loganayaki and R. B. Kumar, "Permanent magnet synchronous motor for electric vehicle applications," in *Proc. 5th Int. Conf. Adv. Comput. Commun. Syst. (ICACCS)*, Sathyamangalam, India, Mar. 2019, pp. 1064–1069.

[4] A. D. Anderson, N. J. Renner, Y. Wang, S. Agrawal, S. Sirimanna, D. Lee, A. Banerjee, K. Haran, M. J. Starr, and J. L. Felder, "System weight comparison of electric machine topologies for electric aircraft propulsion," in *Proc. AIAA/IEEE Electr. Aircr. Technol. Symp. (EATS)*, Cincinnati, OH, USA, Jul. 2018, pp. 1–16.

[5] J. K. Nøland, M. Leandro, J. A. Suul, and M. Molinas, "High-power machines and starter-generator topologies for more electric aircraft: A technology outlook," *IEEE Access*, vol. 8, pp. 130104–130123, 2020.

[6] *Commission Regulation (EU) 2021/341*, Off. J. Eur. Union, Strasbourg, France, 2021.

[7] A. Soualmi, F. Dubas, D. Depernet, A. Randria, and C. Espanet, "Study of copper losses in the stator windings and PM eddy-current losses for PM synchronous machines taking into account influence of PWM harmonics," in *Proc. 15th Int. Conf. Electr. Mach. Syst. (ICEMS)*, Sapporo, Japan, Oct. 2012, pp. 1–5.

[8] A. Mlot, M. Lukaniszyn, and M. Korkosz, "Analysis of end-winding proximity losses in a high-speed PM machine," *Arch. Electr. Eng.*, vol. 65, no. 2, pp. 249–261, Jun. 2016.

[9] X. Chen, H. Fang, D. Li, R. Qu, X. Fan, and H. Hu, "Suppression of winding AC losses in high-speed permanent magnet machines by novel transposition technologies," in *Proc. IEEE Energy Convers. Congr. Expo. (ECCE)*, Vancouver, BC, Canada, Oct. 2021, pp. 4539–4545.

[10] R. Wrobel and B. Mecrow, "A comrephensive review of additive manufacturing in construction of electrical machines," *IEEE Trans. Energy Convers.*, vol. 35, no. 2, pp. 1054–1064, Jun. 2020.

[11] M. Gröninger, F. Horch, A. Kock, M. Jakob, and B. Ponick, "Cast coils for electrical machines and their application in automotive and industrial drive systems," in *Proc. 4th Int. Electr. Drives Prod. Conf. (EDPC)*, Nuremberg, Germany, Sep. 2014, pp. 1–7.

[12] J.-W. Chin, K.-S. Cha, E.-C. Lee, S.-H. Park, J.-P. Hong, and M.-S. Lim, "Design of PMSM for EV traction using MSO coil considering AC resistance according to current density and parallel circuit," in *Proc. IEEE Vehicle Power Propuls. Conf. (VPPC)*, Hanoi, Vietnam, Oct. 2019, pp. 1–6.

[13] M. Linnemann, M. Bach, V. Psyk, M. Werner, M. Gerlach, and N. Schubert, "Resource-efficient, innovative coil production for increased filling factor," in *Proc. 9th Int. Electr. Drives Prod. Conf. (EDPC)*, Esslingen, Germany, Dec. 2019, pp. 1–5.

[14] G. Burnand, A. Thabuls, D. M. Araujo, and Y. Perriard, "Novel optimised shape and topology for slotless windings in BLDC machines," *IEEE Trans. Ind. Appl.*, vol. 56, no. 2, pp. 1275–1283, Mar. 2020.

[15] J. D. Pollock and C. R. Sullivan, "Loss models for shaped foil windings on low-permeability cores," in *Proc. IEEE Power Electron. Spec. Conf.*, Rhodes, Greece, Jun. 2008, pp. 3122–3128.

[16] C. R. Sullivan, J. D. McCurdy, and R. A. Jensen, "Analysis of minimum cost in shape-optimized litz-wire inductor windings," in *Proc. IEEE 32nd Annu. Power Electron. Specialists Conf.*, Vancouver, BC, Canada, Jun. 2001, pp. 1473–1478.

[17] T. Nomura, C.-M. Wang, K. Seto, and S. W. Yoon, "Planar inductor with quasi-distributed gap core and busbar based planar windings," in *Proc. IEEE Energy Convers. Congr. Expo.*, Denver, CO, USA, Sep. 2013, pp. 3706–3710.

[18] A. Starodubov, I. Bakhteev, I. Kozhevnikov, S. Molchanov, T. Amanov, V. Galushka, A. Serdobintsev, and N. Ryskin, "Studies on additive microfabrication of the millimeter-band components by LCD 3D printing and magnetron sputtering," in *Proc. 24th Int. Vac. Electron. Conf. (IVEC)*, Chengdu, China, Apr. 2023, pp. 1–2.

[19] F. Lorenz, J. Rudolph, and R. Werner, "High temperature operation and increased cooling capabilities of switched reluctance machines using 3D printed ceramic insulated coils," in *Proc. IEEE Transp. Electrific. Conf. Expo. (ITEC)*, Long Beach, CA, USA, Jun. 2018, pp. 400–405.

[20] S. Debnath, S. Kunar, S. Anasane, and B. Bhattacharyya, "Non-traditional micromachining processes: Opportunities and challenges," in *Non-Traditional Micromachining Processes*. Cham, Switzerland: Springer, 2017, pp. 1–59.

[21] F. Lorenz, J. Rudolph, and R. Wemer, "Design of 3D printed high performance windings for switched reluctance machines," in *Proc. 13th Int. Conf. Electr. Mach. (ICEM)*, Alexandroupoli, Greece, Sep. 2018, pp. 2451–2457.

[22] BMW AG. (Nov. 2019). *Additive Manufacturing: 3D Printing to Perfection*. [Online]. Available: https://www.bmw.com/en/innovation/3d-print.html

[23] N. Simpson, D. J. North, S. M. Collins, and P. H. Mellor, "Additive manufacturing of shaped profile windings for minimal AC loss in electrical machines," *IEEE Trans. Ind. Appl.*, vol. 56, no. 3, pp. 2510–2519, May 2020.

[24] F. Wu, A. M. El-Refaie, and A. Al-Qarni, "Additively manufactured hollow conductors integrated with heat pipes: Design tradeoffs and hardware demonstration," *IEEE Trans. Ind. Appl.*, vol. 57, no. 4, pp. 3632–3642, Jul. 2021.

[25] I. L. Acevedo, M. Osama, D. Filusch, and H.-G. Herzog, "Design of shaped electric machine windings to reduce ohmic losses," in *Proc. 13th Int. Electr. Drives Prod. Conf. (EDPC)*, Regensburg, Germany, Nov. 2023, pp. 1–8.

[26] F. J. Rudolph, M. Wegelt, and R. Werner, "3D printed high performance windings—Prototypes and testing in a three phase SRM, VDE," in *Proc. Electromech. Drive Syst.; ETG Symp.*, 2022, pp. 123–127.

[27] A. Acquaviva, S. Skoog, and T. Thiringer, "Design and verification of in-slot oil-cooled tooth coil winding PM machine for traction application," *IEEE Trans. Ind. Electron.*, vol. 68, no. 5, pp. 3719–3727, May 2021.

[28] F. Wu and A. M. El-Refale, "Investigation of an additively-manufactured modular permanent magnet machine for high specific power design," in *Proc. IEEE Energy Convers. Congr. Expo. (ECCE)*, Baltimore, MD, USA, Sep. 2019, pp. 777–784.

[29] M.-S. Kim, S.-H. Lee, H.-J. Moon, and C.-E. Kim, "Multi-objective geometric optimal design of industrial high-voltage induction motor for cost reduction," in *Proc. IEEE Transp. Electrific. Conf. Expo, Asia–Pacific (ITEC Asia–Pacific)*, Chiang Mai, Thailand, Nov. 2023, pp. 1–8.

[30] N. Riviere, M. Stokmaier, and J. Goss, "An innovative multi-objective optimization approach for the multiphysics design of electrical machines," in *Proc. IEEE Transp. Electrific. Conf. Expo (ITEC)*, Chicago, IL, USA, Jun. 2020, pp. 691–696.

[31] E. Roshandel, N. Ertugrul, A. Mahmoudi, and S. Kahourzade, "Design optimisation of a high power density electric machine using soft magnetic composites," in *Proc. 32nd Australas. Universities Power Eng. Conf. (AUPEC)*, Adelaide, SA, Australia, Sep. 2022, pp. 1–6.

[32] B. Cheong, P. Giangrande, X. Zhang, M. Galea, P. Zanchetta, and P. Wheeler, "Evolutionary multiobjective optimization of a system-level motor drive design," *IEEE Trans. Ind. Appl.*, vol. 56, no. 6, pp. 6904–6913, Nov. 2020.

[33] K. Diao, X. Sun, G. Lei, Y. Guo, and J. Zhu, "Multimode optimisation of switched reluctance machines in hybrid electric vehicles," *IEEE Trans. Energy Convers.*, vol. 36, no. 3, pp. 2217–2226, Sep. 2021.

[34] G. Petrelli, S. Nuzzo, D. Barater, T. Zou, G. Franceschini, and C. Gerada, "Preliminary sensitivity analysis and optimisation of a wound field synchronous motor for traction applications," in *Proc. AEIT Int. Conf. Electr. Electron. Technol. Automot. (AEIT AUTOMOTIVE)*, Modena, Italy, Jul. 2023, pp. 1–6.

[35] T. Helmholdt-Zhu and H. Borcherding, "Investigations on the influences of winding positions and rise times on the winding isolation system within the line-end coil under fast rising impulse voltages," in *Proc. 23rd Eur. Conf. Power Electron. Appl. (EPE ECCE Europe)*, Ghent, Belgium, Sep. 2021, pp. 1–10.

[36] S. N. Tripathy, S. Kundu, and A. Pradhan, "Multi-objective optimization technique based design of squirrel cage induction motor," in *Proc. 2nd Int. Conf. Power Electron. IoT Appl. Renew. Energy Control (PARC)*, Mathura, India, Jan. 2022, pp. 1–6.

[37] M. Lu, G. Domingues-Olavarría, F. J. Márquez-Fernández, H. Bydén, and M. Alaküla, "Optimization of induction machine design for electric vehicle powertrain," in *Proc. IEEE Int. Electr. Mach. Drives Conf. (IEMDC)*, San Francisco, CA, USA, May 2023, pp. 1–6.

[38] F. Kiani and H. Tahanian, "A new methodology for design optimization of interior permanent magnet motors for electric vehicle applications," in *Proc. 3rd Int. Conf. Electr. Mach. Drives (ICEMD)*, Tehran, Iran, Dec. 2023, pp. 1–5.

[39] F. Yu, H. Chen, W. Yan, V. F. Pires, J. F. A. Martins, P. Rafajdus, A. Musolino, L. Sani, M. P. Aguirre, M. A. Saqib, M. Orabi, and X. Li, "Design and multiobjective optimization of a double-stator axial flux SRM with full-pitch winding configuration," *IEEE Trans. Transport. Electrific.*, vol. 8, no. 4, pp. 4348–4364, Dec. 2022.

[40] J. Li, Y. Li, and Y. Wang, "Fuzzy inference NSGA-III algorithm-based multi-objective optimization for switched reluctance generator," *IEEE Trans. Energy Convers.*, vol. 36, no. 4, pp. 3578–3581, Dec. 2021.

[41] M. Shang and J. Liu, "Multi-objective optimization of high power density motor based on metamodel of optimal prognosis," in *Proc. IECON - 49th Annu. Conf. IEEE Ind. Electron. Soc.* Singapore: IEEE, Oct. 2023, pp. 1–6.

[42] D. Wei, H. He, and J. Li, "A computationally efficiency optimal design for a permanent magnet synchronous motor in hybrid electric vehicles," in *Proc. IEEE 9th Int. Power Electron. Motion Control Conf. (IPEMC-ECCE Asia)*, Nanjing, China, Nov. 2020, pp. 43–47.

[43] A. Gneiting, M. Waldhof, and N. Parspour, "A systematic design methodology based on data clustering for automotive drive cycle oriented optimization of electrically excited synchronous machines," in *Proc. IEEE 7th Southern Power Electron. Conf. (SPEC)*, Nadi, Fiji, Dec. 2022, pp. 1–8.

[44] P. Lindh, H. Jussila, J. Pyrhonen, A. Parvianen, and M. Niemela, "Concentrated wound PM motors with semi-closed slots and with open slots," *Int. Rev. ELectrical Eng. (IREE)*, vol. 5, no. 2, pp. 491–497, 2010.

[45] J. Pyrhonen, T. Jokinen, and V. Hrabovocova, *Design of Rotating Electrical Machines*, 2nd ed., Hoboken, NJ, USA: Wiley, 2014, pp. 275–276.

[46] D. Liang, Z. Q. Zhu, Y. Zhang, J. Feng, S. Guo, Y. Li, J. Wu, and A. Zhao, "A hybrid lumped-parameter and two-dimensional analytical thermal model for electrical machines," *IEEE Trans. Ind. Appl.*, vol. 57, no. 1, pp. 246–258, Jan. 2021.

[47] L. Jin, Y. Mao, X. Wang, L. Lu, and Z. Wang, "A model-based and data-driven integrated temperature estimation method for PMSM," *IEEE Trans. Power Electron.*, vol. 39, no. 7, pp. 8553–8561, Jul. 2024.

[48] R. Reddivari, V. Savant, and H. Eldeeb, "A model-based lumped parameter thermal network for online temperature estimation of IPMSM in automotive applications," in *Proc. IEEE Int. Transp. Electrific. Conf. (ITEC-India)*, Chennai, India, Dec. 2023, pp. 1–6.

[49] A. A. S. Leao, F. M. B. Toledo, J. F. Oliveira, M. A. Carravilla, and R. Alvarez-Valdés, "Irregular packing problems: A review of mathematical models," *Eur. J. Oper. Res.*, vol. 282, no. 3, pp. 803–822, May 2020.

[50] X. Zhao, Z. Sun, and Y. Xu, "Multi-objective optimization design of permanent magnet synchronous motor based on genetic algorithm," in *Proc. 2nd Int. Conf. Mach. Learn., Big Data Bus. Intell. (MLBDBI)*, Taiyuan, China, Oct. 2020, pp. 405–409.

[51] A. Saltelli, M. Ratto, T. Andres, F. Campolongo, J. Cariboni, D. Gatelli, M. Saisana, and S. Tarantola, *Global Sensitivity Analysis: The Primer*. Chichester, U.K.: Wiley, 2008.

[52] *Methods for Optimisation and Robustness Analysis*, Dynardo GmbH, Weimar, Germany, 2020.

[53] P. Asef, M. Denai, J. J. H. Paulides, B. R. Marques, and A. Lapthorn, "A novel multi-criteria local Latin hypercube refinement system for commutation angle improvement in IPMSMs," *IEEE Trans. Ind. Appl.*, vol. 59, no. 2, pp. 1588–1602, Mar. 2023.

[54] T. Most and J. Will, "Metamodel of optimal prognosis—An automatic approach for variable reduction and optimal meta-model selection," in *Proc. Weimar Optim. Stochastic Days 5.0*, Weimar, Germany, 2008, pp. 1–21.

[55] J. Shier and P. Bourke, "An algorithm for random fractal filling of space," *Comput. Graph. Forum*, vol. 32, no. 8, pp. 89–97, Dec. 2013.

[56] L. Stoyanov, V. Lazarov, Z. Zarkov, and E. Popov, "Influence of skin effect on stator windings resistance of AC machines for electric drives," in *Proc. 16th Conf. Electr. Mach., Drives Power Syst. (ELMA)*, Varna, Bulgaria, Jun. 2019, pp. 1–6.

[57] A. Selema, M. N. Ibrahim, R. Sprangers, and P. Sergeant, "Effect of using different types of magnet wires on the AC losses of electrical machine windings," in *Proc. IEEE Int. Electr. Mach. Drives Conf. (IEMDC)*, Hartford, CT, USA, May 2021, pp. 1–5.

[58] A. Payne, "Skin effect, proximity effect and the resistance of circular and rectangular conductors," A. P. Associates, Chennai, India, Tech. Rep., 2021, pp. 1–33. [Online]. Available: https://www.researchgate.net/publication/351306996_SKIN_EFFECT_PROXIMITY_EFFECT_AND_THE_RESISTANCE_OF_CIRCULAR_AND_RECTANGULAR_CONDUCTORS

[59] G. S. Dimitrakakis and E. C. Tatakis, "High-frequency copper losses in magnetic components with layered windings," *IEEE Trans. Magn.*, vol. 45, no. 8, pp. 3187–3199, Aug. 2009.

[60] P. M. Lindh, H. K. Jussila, M. Niemela, A. Parviainen, and J. Pyrhonen, "Comparison of concentrated winding permanent magnet motors with embedded and surface-mounted rotor magnets," *IEEE Trans. Magn.*, vol. 45, no. 5, pp. 2085–2089, May 2009.
[61] H. Mirahki, K. Atallah, L. Rodrigues, and T. Cawkwell, "Concept design and optimization methodology of a wound field synchronous motor for commercial vehicle applications," in *Proc. IEEE Energy Convers. Congr. Expo. (ECCE)*, Nashville, TN, USA, Oct. 2023, pp. 4330–4337.
[62] A. Al-Qarni and A. El-Refaie, "Semi-stranded and shaped-profile hollow additively manufactured coils with integrated heat pipes for all-electric aircraft motors," in *Proc. IEEE Energy Convers. Congr. Expo. (ECCE)*, Nashville, TN, USA, Oct. 2023, pp. 4516–4523.

JOHN MCKAY (Member, IEEE) received the M.Eng. degree in electronics and electrical engineering from the University of Strathclyde, Glasgow, U.K., in 2015.

He is currently a Ph.D. Researcher and an Engineer with the Design, Manufacturing and Management Department, University of Strathclyde, and the Advanced Forming Research Centre. His research belongs to the FEMM hub, the Future Electric Machines Manufacturing hub an EPSRC funded venture with NMIS, the National Manufacturing Institute Scotland. His research interests include improvement of performance of electrical machines through the use of advanced multi-physics, algorithmic design processes and novel manufacturing techniques utilizing additive manufacturing of active components for potential deployments in automotive, aerospace, transportation, and manufacturing.

JILL MISCANDLON received the B.Sc. (Hons.) and Ph.D. degrees in mathematics from the University of Strathclyde, before joining the Advanced Forming Research Centre, a technical centre within the National Manufacturing Institute Scotland. She worked for six years leading large-scale CR&D projects on novel forming processes, such as flow forming and spinning, including the strategic affordable manufacturing in U.K. through leading environmental technologies (SAMULET) and manufacturing portfolio projects. She is currently leading two grand challenges for the EPSRC's Future Electrical Machines Manufacturing Hub, including developing the work package around sustainable manufacture and circular economy of electrical machines. Her research interests include manufacturing innovations for electrical machines, near net shape forming technologies, and sustainable manufacture and design.

TATYANA KONKOVA is currently a Senior Lecturer with the University of Strathclyde (UoS), and leading the Materials Processing Team at the Department of Design, Manufacturing and Engineering Management (DMEM), UoS. She has significant expertise in advanced materials characterization techniques, materials thermo-mechanical behaviors, electro-pulse treatment, electrodeposition, and additive manufacturing. She has over 50 highly cited publications and has authored numerous industrial reports. She has led research and knowledge exchange programs focused on materials behavior during forging, forming, and processing. She is a Chartered Engineer and a member of IMechE and The Scottish Association for Metals (SAM) Council, and a Fellow of IOM3.